

DEVELOPMENT AND EVALUATION OF A NEW CONCEPT OF HIGH EFFICIENCY PASSIVE AUTOCATALYTIC RECOMBINERS

Philippe Chantereau¹, Sébastien Diaz², Antoine Maros³, Alexandre Bleyer⁴, Ahmed Bentaib⁵

¹ Technological Development Director, Nuvia Protection, Morestel, France
(philippe.chantereau@nuvia.com)

² CEO, Nuvia Protection, Morestel, France

³ Design & Research Engineer, Nuvia Protection, Morestel, France

⁴ Research Engineer, IRSN, PSN-RES/SAM, Fontenay-aux-Roses, France

⁵ Expert, IRSN, PSN-RES/SAM, Fontenay-aux-Roses, France

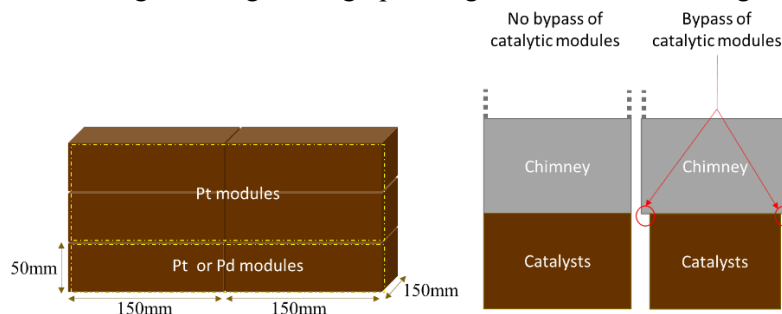
INTRODUCTION

During a severe accident (SA) in a light water nuclear reactor, large amounts of burnable gases (H₂ and CO) could be generated and released into the containment during reactor core degradation and molten corium/concrete interaction (MCCI) phases. This could subsequently raise a combustion hazard.

To prevent gas explosion hazard, most NPPs have already adopted or are adopting strategies (some of them as a result of the stress tests after the Fukushima accident) based on the use of Passive Autocatalytic Recombiners (PARs). PARs are entirely passive safety devices, converting hydrogen and carbon monoxide into water and carbon dioxide by means of an exothermal catalytic surface reaction. Typically, several dozen devices are installed inside the LWR containments with the objective to fulfill the adopted requirements in each country.

Nevertheless, and despite the PARs implementation, deterministic and probabilistic assessment show that flammable mixture liable to lead to local flame acceleration phenomena cannot always be excluded at all points of the containment. To overcome this limitation, NUZIA is developing the PARHE recombiner concept with the objective of high conversion efficiency and lower start-up concentration.

The PARHE concept relies on honeycomb catalytic modules. The predesign allowed them to be piled-up if the numerical and experimental studies demonstrated benefits. Configurations with up to two stacks of three blocks were considered in the experimental and numerical studies. The full-scale configuration is illustrated on figure 1, with a chimney of an undetermined length in the predesign. The influence of a bypass, according to the right-end graph of figure 1, was also investigated in the simulations.



EXPERIMENTAL ASSESSMENT OF PARHE PERFORMANCES

Forced flow experiments

Experiments have been conducted to assess the behaviour of different technologies of catalyst that would later be integrated in the full-scale PAR. The experimental campaign had been conducted in collaboration with Jülich Forschungszentrum on their REKO experimental platform (Reinecke, May 16–18, 2006.). The catalysts considered are built with a honeycomb structure, which drafts important exchange surfaces in reduced space. Since the recombination reaction occurs on the catalyst's surface, such a structure can bring important benefits in terms of operation range compared to metal-sheet based PARs. The first phase consisted of forced-flow experiments to evaluate different catalysers' performances when subject to controlled flow characteristics. It was done on the REKO-1 experimental setup, using recut catalytic samples to fit the test rig's dimensions.

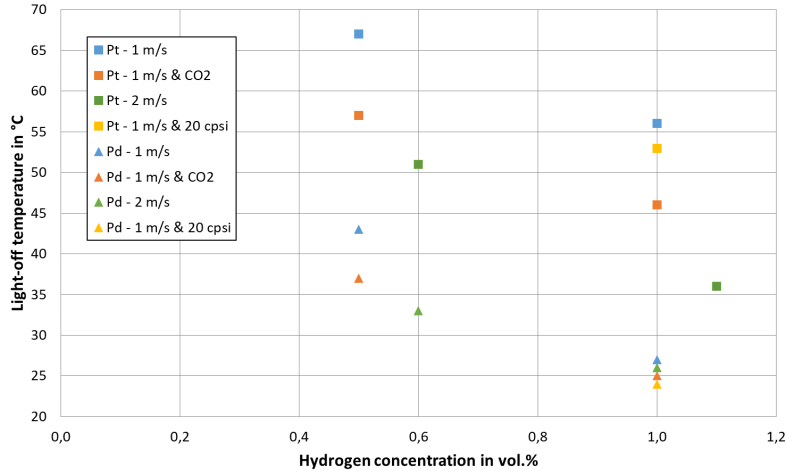
The test matrix included different honeycomb mesh size (20 cells per square inch and 50 cps), different materials (Pt and Pd), inlet velocities (1m/s and 2m/s), and hydrogen inlet concentrations (0.5%vol and 1 vol%). The influence of carbon dioxide has also been briefly explored. The main goal of the forced-flow tests was to determine the light-off conditions of all the catalytic modules we considered, as well as their efficiency, to later orient the choice of the modules to assess in natural flow conditions.

To determine the light-off conditions, two different hydrogen concentrations of 0.5 %vol and 1%vol have been explored. For both cases, tests started at ambient temperature and a corresponding relative humidity of 70%. If no start-up was observed after a given time, the inlet temperature was progressively increased, thus decreasing the ambient humidity in the meantime, until light-off was observed. Once the reaction started, steady-state recombination rate and efficiency were recorded.

The presence of carbon dioxide in the atmosphere facilitated the light-off, since it consistently lowered the start-up temperature for a given configuration. Consequently, it was not considered in the rest of the experimental campaigns, as it did not negatively impact the catalysers' performances.

The light-off tests also demonstrated better performances for palladium modules, lighting-on at ambient temperature at 1%vol H₂, and under 45°C at 0.5%vol H₂. In contrast, platinum catalysts showed better recombination performances as highlighted in Figure 2 for 1m/s inlet velocities, although the relative improvement is significantly reduced for 2m/s inlet velocity. The efficiency also decreases with an increase in velocity since the hydrogen crosses the catalytic module in a shorter time span.

The slight modification in hydrogen concentration from 0.5 to 0.6%vol and from 1 to 1.1%vol is due to a limitation in the test rig which leads to inject pure nitrogen along with ambient air to reach the target of 2m/s flow velocity. The quantity of hydrogen going through the recombiner in each time span remained unchanged from the equivalent 1m/s tests. Based upon these results, the natural convection campaign test matrix aimed at determining the natural flow velocity under certain hydrogen concentrations, and to assess the impact of various chimney lengths. We also considered piling-up catalytic modules to combine palladium modules' lower starting conditions to platinum modules' higher recombination rates.



Natural flow experiments

The natural flow experiments were performed on the REKO-4 facility. Figure 4 illustrated the estimation of flow velocities for the considered configurations. While the medium chimney seems to have no significant impact on the recombination, the larger chimney drafts significantly more air into the catalysts. Interestingly, the smaller mesh size catalysts show worse performances than their larger counterparts, as opposed to their behaviour in forced-flow conditions. Piling modules also led to higher pressure drops in the module's channels, and thus showed lower performances than single modules.

All the modules were able to light-off and operate at 1%vol H₂ at room temperature in natural flow conditions, although platinum catalysts showed higher start-up regardless of relative humidity. Moreover, 0.5%vol H₂ concentration was identified as limit to recombiners' operation. It appeared throughout the different experiments that hydrogen could not diffuse to the catalyst surfaces sufficiently to establish a chimney flow. Nonetheless, catalysts' surface temperature showed a slow increase when exposed to 0.5%vol H₂ atmosphere, highlighting that a recombination reaction still occurred at the catalyst surface.

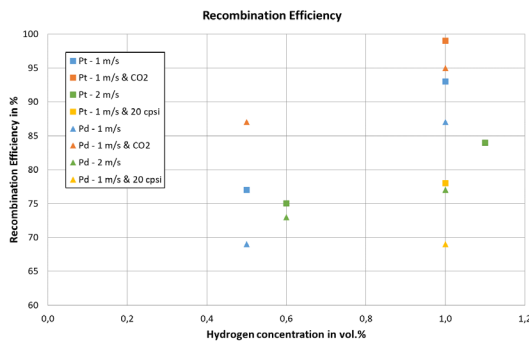


Figure 3. Recombination efficiency of the various modules

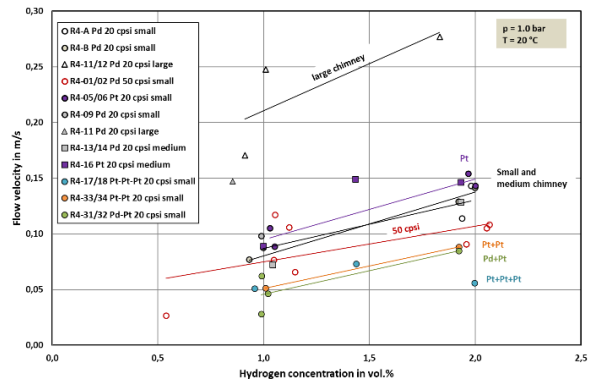


Figure 4. Flow velocities in the test rig for various configurations

The experimental results, illustrated in Figure 3 and Figure 4, allowed us to determine the catalyst's front area and the recombiner's height needed depending on the working conditions, to later validate a full-scale model experimentally.

NUMERICAL ESTIMATION OF PERFORMANCES

Single channel simulations & model optimization

To anticipate further changes in the recombiners' design, a numerical model has been set up to mimic the experiments as faithfully as achievable. If the numerical studies prove to give reliable predictions, they could be used later to evaluate the impact on performances of various modifications to the initial design, which allows to test a much larger number of configurations than experimental campaigns.

The numerical study has been conducted in collaboration with IRSN using their in-house CFD code SPARK (Meynet, 2014), as well as the commercial ANSYS FLUENT (Ansys Fluent 19.2, (2018), Theory Guide, ANSYS, Inc). The focus was mainly to investigate the behaviour of stacks of catalytic modules.

The preliminary step was to correctly tweak the chemical surface reaction occurring on the catalyst's surface. To do so, the model was first focused on modelling a single catalyst channel with an axisymmetric geometry and implement the reaction mechanisms, both on the surface and in the gas phase. In a first time, the reactions were implemented according to Table 1 following previous works (Warnatz, 1996 and Deutschmann, 1996). Simulations using these surface chemistry mechanisms showed different light-off behaviour compared to experiments. Particularly, the light-off temperature was highly over-estimated compared to the experimental results. The adsorption reaction (1) in table 1 was adapted to better fit the experimental results in that aspect.

The same chemistry model being implemented in both FLUENT and SPARK, a comparative study has been conducted to evaluate the performances of both solvers. Results showed that FLUENT consistently predicted lower temperatures for all the different input conditions considered. It goes with lower predicted recombination rates and higher hydrogen concentrations in the output, since the only heat sources are the chemical reactions occurring.

Table 1. Chemical reactions implemented in SPARK and Fluent CFD codes

Num.	Reaction	A	B	E _a (cal/mol)
1	H + O ₂ ⇌ O + OH	2.00 × 10 ¹⁴	0.00	16 802.10
2	O + H ₂ ⇌ H + OH	2.06 × 10 ⁰⁴	2.67	6 285.85
3	H ₂ + OH ⇌ H ₂ O + H	1.00 × 10 ⁰⁸	1.60	3 298.28
4	OH + OH ⇌ O + H ₂ O	1.50 × 10 ⁰⁹	1.14	100.38
5	H + H + M ⇌ H ₂ + M H ₂ O/6.5/ O ₂ /0.4 N ₂ /0.4	1.80 × 10 ¹⁸	-1.00	0.00
6	O + O + M ⇌ O ₂ + M H ₂ O/6.5/ O ₂ /0.4 N ₂ /0.4	2.90 × 10 ¹⁷	-1.00	0.00
7	H + OH + M ⇌ H ₂ O + M H ₂ O/6.5/ O ₂ /0.4 N ₂ /0.4	2.20 × 10 ²²	-2.00	0.00
8	H + O ₂ + M ⇌ HO ₂ + M H ₂ O/6.5/ O ₂ /0.4 N ₂ /0.4	2.30 × 10 ¹⁸	-0.80	0.00
9	HO ₂ + H ⇌ H ₂ + O ₂	2.50 × 10 ¹³	0.00	693.12
10	HO ₂ + H ⇌ 2OH	1.50 × 10 ¹⁴	0.00	1 003.82
11	HO ₂ + H ⇌ H ₂ O + O	3.00 × 10 ¹³	0.00	1 720.84
12	HO ₂ + O ⇌ OH + O ₂	1.80 × 10 ¹³	0.00	-406.31
13	HO ₂ + OH ⇌ H ₂ O + O ₂	6.00 × 10 ¹³	0.00	0.00
14	2 HO ₂ ⇌ H ₂ O ₂ + O ₂	2.50 × 10 ¹⁴	0.00	-1 242.83
15	2 OH + M ⇌ H ₂ O ₂ + M H ₂ O/6.5/ O ₂ /0.4 N ₂ /0.4	3.25 × 10 ²²	-2.00	0.00
16	H ₂ O ₂ + H ⇌ H ₂ O + OH	1.00 × 10 ¹³	0.00	3 585.09
17	H ₂ O ₂ + H ⇌ H ₂ + HO ₂	1.70 × 10 ¹²	0.00	3 752.39
18	H ₂ O ₂ + O ⇌ OH + HO ₂	2.80 × 10 ¹³	0.00	6 405.35
19	H ₂ O ₂ + OH ⇌ H ₂ O + HO ₂	5.40 × 10 ¹²	0.00	1 003.82

Remarque. Coefficients de la loi d'Arrhenius : $k = A T^B \exp(-E_a/RT)$

Num.	Réaction d'adsorption	s coefficient d'adhésion	
1	H ₂ + 2 Pt ^(s) → 2 H ^(s)	0.046	
2	H + Pt ^(s) → H ^(s)	1.000	
3	O ₂ + 2 Pt ^(s) → 2 O ^(s)	0.070	
4	O + Pt ^(s) → O ^(s)	1.000	
5	H ₂ O + Pt ^(s) → H ₂ O ^(s)	0.750	
6	OH + Pt ^(s) → OH ^(s)	1.000	
Num.	Réaction de recombinaison	A	E _a (kJ/mol)
7	H ^(s) + O ^(s) ⇌ OH ^(s) + Pt ^(s)	3.70 × 10 ²¹	11.5
8	H ^(s) + OH ^(s) ⇌ H ₂ O ^(s) + Pt ^(s)	3.70 × 10 ²¹	17.4
9	2 OH ^(s) ⇌ H ₂ O ^(s) + O ^(s)	3.70 × 10 ²¹	48.2
Num.	Réaction de désorption	A	E _a (kJ/mol)
10	2 H ^(s) → H ₂ + 2 Pt ^(s)	3.70 × 10 ²¹	67.4-6.0σ _H
11	2 O ^(s) → O ₂ + 2 Pt ^(s)	3.70 × 10 ²¹	213.2-60.0σ _O
12	H ₂ O ^(s) → H ₂ O + Pt ^(s)	1.00 × 10 ¹³	40.3
13	OH ^(s) → OH + Pt ^(s)	1.00 × 10 ¹³	192.8

As showed in figure 5, the main difference lies in the prediction of the reaction occurring in the first 20mm of catalyst, where the surface temperature increase is more important. The lower reaction rate in that section then reflects in the hydrogen concentrations difference all along module 1, and the increase in the axial temperature difference in module 2, where the flow is more homogeneous. Nonetheless, both solvers predicted very similar flows. The small difference in performance can be explained by the detailed multi-transport equations implemented in SPARK, compared to FLUENT.

Once the validation step achieved, a parametric study has been conducted on the number and material of catalytic modules for various inlet velocities and hydrogen concentrations as summarized in Table 2.

Table 2. Tested configurations for single modules simulations

Module 3	Pt	Pd	Pt	Inert	Absent	Absent
Module 2	Pt	Pd	Pt	Pt	Pt	Absent
Module 1	Pt	Pd	Pd	Pt	Pt	Pt

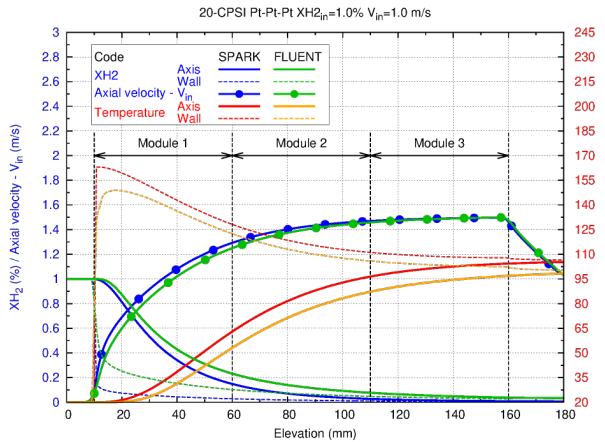


Figure 5. Comparison of FLUENT and SPARK results on the Pt-Pt-Pt configuration.

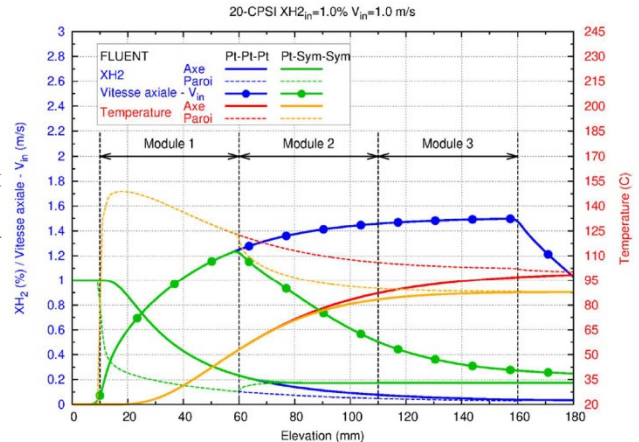


Figure 6. Evolution of the flow characteristics in a catalyst channel

Moreover, hydrogen molar fraction, gas temperature and velocity magnitude, as shown in Figure 7, confirm that for the considered configurations, the catalytic reaction occurs mostly in the first module.

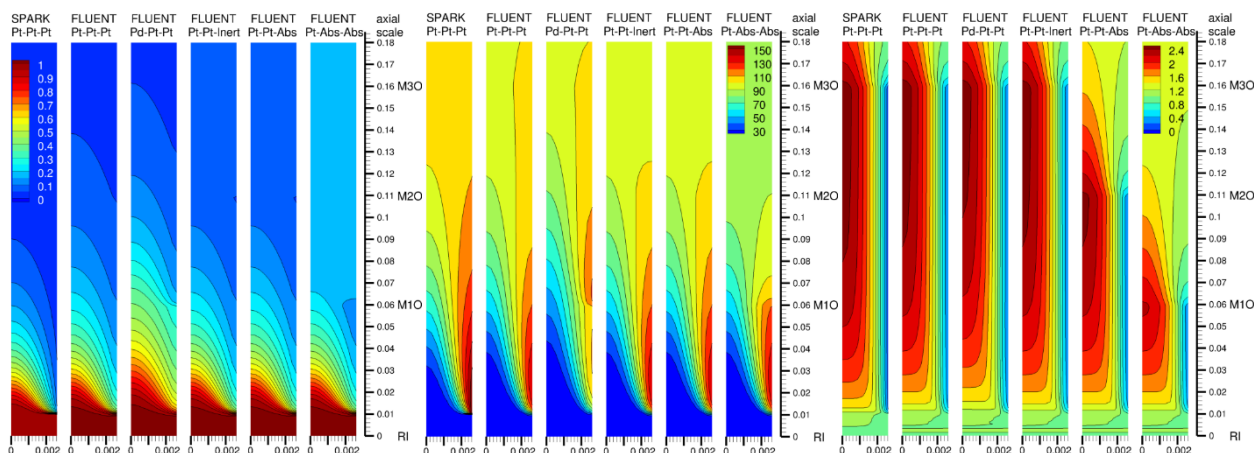


Figure 7. Hydrogen molar fraction (%) fields at the left, temperature (°C) fields at the middle, velocity magnitude (m/s) fields at the right for different configurations (*RI*, stands for *Recombiner Inlet* and *MiO*, for *Module i Outlet*, $i = 1, 2, 3$).

The table 3 summarizes the results for all the different tested configurations for single-channel simulations.

Table 3. Results summary for single-channel simulation results

Configuration	XH2 (%)				Temperature (°C)				Axial Speed (m/s)			
	RI	M1O	M2O	M3O	RI	M1O	M2O	M3O	RI	M1O	M2O	M3O
Pt-Pt-Pt	1.00%	0.15%	0.06%	0.03%	20.0	98.9	99.9	100.3	1.000	1.227	1.257	1.274
Pd-Pd-Pd	1.00%	0.31%	0.17%	0.11%	20.0	85.5	91.9	94.5	1.000	1.183	1.226	1.252
Pd-Pt-Pt	1.00%	0.29%	0.09%	0.04%	20.0	87.7	99.5	100.2	1.000	1.185	1.249	1.272
Pt-Pt-Inert	1.00%	0.15%	0.06%	0.06%	20.0	98.9	99.7	97.3	1.000	1.227	1.257	1.266
Pt-Pt-Absent	1.00%	0.15%	0.06%	0.06%	20.0	98.9	99.6	97.2	1.000	1.227	1.266	1.257
Pt-Absent-Absent	1.00%	0.16%	0.17%	0.17%	20.0	97.7	88.2	88.1	1.000	1.237	1.227	1.227

The analysis of the performed simulations, considering a single catalyst channel, allowed deriving recombination correlation for the various configurations of modules stacks, as shown in the figure 8 below. The full lines represent a complete hydrogen recombination rate and the dotted lines the recombination rate predicted by the codes (SPARK and Fluent). The latter helped developing new correlation expressing hydrogen recombination versus gas inlet velocity, initial temperature and initial gas composition.

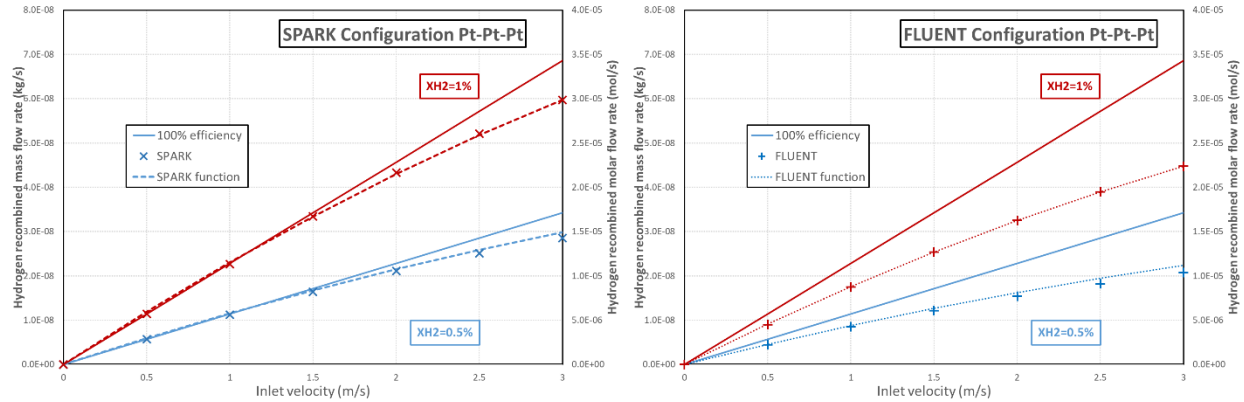


Figure 8. Recombination functions for both FLUENT and SPARK in the case of a Pt-Pt-Pt configuration.

Full-scale simulations

Using the recombination correlation issued from the previous step, a full-scale, two piles of three catalytic modules recombiner has been simulated as shown in figure 9, both with and without a bypass next to the stacks of modules. Two types of simulation have been conducted on that geometry. Firstly, simulations representing only the recombiner in forced-flow, using the recombination correlation based on the performed single-channel simulations results. That setup was called “elementary” in the results. Secondly, simulations representing the recombiner in its environment, in natural-flow conditions where the flow in the recombiner is only induced by the exothermic reaction. That setup was called “global” in the results. In both cases, the catalytic modules were modelled as porous media, where the recombination function was implemented to occur on a single cell layer of the numerical mesh, as shown in figure 9.

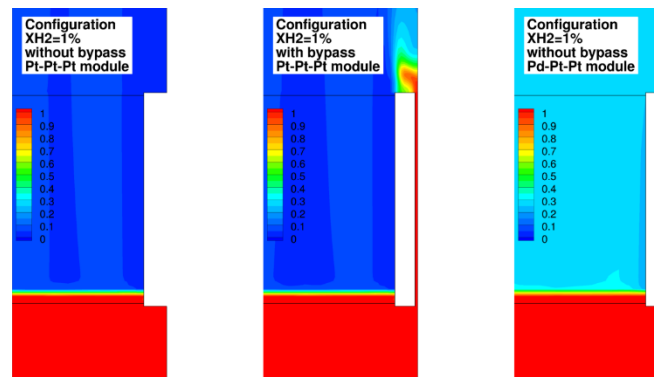


Figure 9. Hydrogen concentration in the full-scale recombiner for elementary setups

Table 4. Full-scale simulations results (RMI stands for Recombiner Module Inlet, RMO Recombiner Module Outlet, RO Recombiner Outlet)

Setup	Geometry	Configuration	XH ₂ (%)			Temperature (°C)			Vertical Speed (m/s)		
			RMI	RMO	RO	RMI	RMO	RO	RMI	RMO	RO
<i>Elementary</i>	No-bypass	Pt-Pt-Pt	1	0.056	0.056	20	97.6	90	1.56	1.99	1.23
<i>Global</i>	No-bypass	Pt-Pt-Pt	1	0.069	0.070	20	96.8	90	1.73	2.21	1.37
<i>Elementary</i>	No-bypass	Pd-Pt-Pt	1	0.286	0.285	20	77.7	72.1	1.56	1.89	1.17
<i>Global</i>	No-bypass	Pd-Pt-Pt	1	0.290	0.291	20	77.4	72.1	1.61	1.94	1.2
<i>Elementary</i>	Bypass	Pt-Pt-Pt	1	0.055	0.066	20	97.7	89.5	1.55	1.97	1.23
<i>Global</i>	Bypass	Pt-Pt-Pt	1	0.068	0.077	20	96.8	89.7	1.72	2.19	1.36

A quick comparison of the ‘elementary’ results presented in table 4 with the single-channel results shows good correlation for the no-bypass geometry. Natural flow simulations generally demonstrate lower efficiencies, which results from the higher flow speed in the modules. The bypass geometry shows similar performances for the modules themselves, as the RMO concentrations are like the no-bypass elementary simulations. The RO concentration increase is likely caused by the hydrogen going through the bypass, which does not participate in the recombination.

Detailed channels flow simulation

To check model validity based on the use of porous media and the developed recombination correlation, confirmatory simulations considering all catalysts’ channels have been performed. The results show small difference in the predicted gas temperature in the inner part of the modules. Unsurprisingly, the detailed simulations allow for a better understanding of the flow’s behaviour. Especially, it highlights higher gas temperature inside of the catalytic modules, which can be explained partly by the heat transfers which favours cooling the outer channels, while the centre channels will be heated by adjacent channels as well as the catalytic reaction occurring in the channel itself.

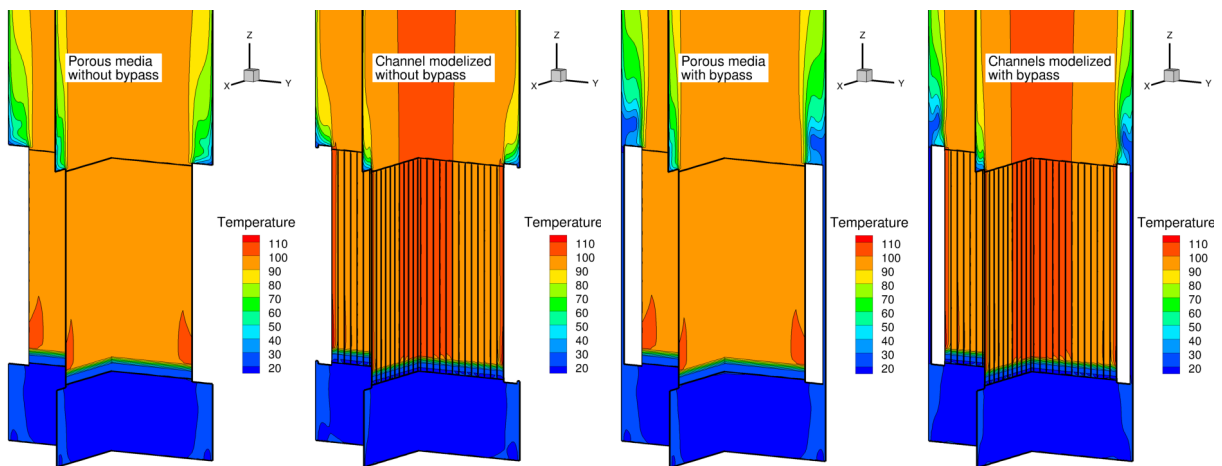


Figure 10. Comparison of the temperature profiles between porous media and real channels simulations

Table 5. Evaluation of the influence of channels simulation on performance prediction

Model	Geometry	Configuration	XH ₂ (%)			Temperature (°C)			Vertical speed (m/s)		
			RMI	RMO	RO	RMI	RMO	RO	RMI	RMO	RO
Elementary	No-bypass	Pt-Pt-Pt	1	0.056	0.056	20	97.6	90	1.56	1.99	1.23
Channels	No-bypass	Pt-Pt-Pt	1	0.077	0.080	20	99.4	91.6	1.49	1.87	1.24
Elementary	Bypass	Pt-Pt-Pt	1	0.055	0.066	20	97.7	89.5	1.55	1.97	1.23
Channels	Bypass	Pt-Pt-Pt	1	0.075	0.103	20	99.7	90.3	1.46	1.83	1.24

The results compiled in table 5 show relative coherence between the two types of setups. Interestingly, when computing the complete reaction on the channels' interior surface, the reaction's efficiency decreased as well as the flow velocity. Both results tend to be more coherent with experimental behaviour, although the simulation was still in forced-flow conditions. The numerical cost of the simulations computing the channels' details was significantly increased compared to porous media. As a result, such setups must be used in specific cases and can hardly be implemented for parametric studies.

COMPARISON OF NUMERICAL AND EXPERIMENTAL RESULTS

As final step, we compare numerical and experimental results for a single platinum module in forced flow condition, at 1% H₂ and 1m/s inlet velocity. The results show good agreement between experiments and simulations. It hints that the details of the chemical reaction are well implemented in the solver for the steady-state performances.

Table 6. Comparison of numerical and experimental results for forced flow, 1% H₂, 1m/s, single platinum module

	v_{inlet} (m/s)	$T_{s,bot}$ (°C)	$T_{s,top}$ (°C)	Efficiency	H _{2,in} (%vol)	H _{2,out} (%vol)
IRSN (FLUENT)	1	130	140	82%	1	0,18
Jülich (REKO-1)	1,14	116	122	78%	1	0,22

Where v_{inlet} is the mean velocity at the inlet of the module, $T_{s,bot/top}$ are respectively the surface temperatures at the bottom and at the top of the catalyst, and H_{2,in/out} are respectively the molar fraction of hydrogen at the inlet of the recombiner and at its outlet.

Experiments showed that it was impossible for three-modules recombiners to light-off as evidenced in the simulations, thus showing that light-off prediction must be further tweaked to reproduce real-world behaviour. Predicted flow velocities for three modules piles were also significantly higher than experimentally observed, and thus predicted much higher recombination rates than observed experimentally. It can have several explanations. The most impactful difference between experimental and numerical setups is the fact that we consider for numerical simulations that the modules' channels are perfectly aligned. In real life, they might be slightly offset, since the 150mm of channel length is not achieved through a single module but through stacking three modules of 50mm height. Furthermore, at the interface between two catalytic modules, it is very likely for the flow to slightly expand in the interstices since the modules' surface is not perfectly even. These two phenomena are likely to have great impacts on the flow inside the channels as well as the pressure drop along the three modules. To improve simulations predictions, it would require investigating experimentally the pressure drops along the three modules. However, experiments pointed that piling modules causes a drop in performances. For that reason, it was chosen to abandon the initial idea of piling modules and to only use single catalytic blocks.

Experiments also highlighted that for 0.5% H₂ concentration the catalytic reaction occurred but at such low rates that it could not induce a chimney flow for natural flow working conditions. In forced-flow conditions though, the experiments also managed to establish steady-state reactions, which is coherent with SPARK and FLUENT behaviour.

CONCLUSION

Experiments demonstrated the important shift in behaviour that can occur between forced flow and natural flow conditions. Forced flow experiments underlined lower light-off temperature for palladium and higher recombination rates for platinum, which suggested an interest in mixing both materials by piling-up catalytic modules. Natural convection experiments, on the contrary, showed little difference in recombination rates between the two materials, all other things being equal. In contrast, the better light-off behaviour of palladium modules was confirmed, with light-off observed in wet atmospheres at ambient temperature and 1%vol hydrogen concentration.

More important, experiments demonstrated a performance drop for piled-up modules that simulations could not predict and oriented the final configuration to single catalytic modules. It also evidenced over-estimated flow velocities in simulations and differences in light-off prediction, which will be useful to finely tune the numerical model before using it for further design optimizations. It is likely that simulating single modules recombiners in natural flow conditions will already draw more realistic results, since the numerical geometry will better represent the real single module than it represented the three separate modules as a monolith.

As is, the numerical model already proved good correlation in terms of chemical kinematics, with single module, forced flow simulation results being especially close to the experimental observations. Computing the detailed flow inside the catalysts' channels can bring a better understanding of the phenomena at stake but reveals to be numerically costly. As such, it must be used sparingly to verify porous media tuning.

Simulations also allowed to understand the harmful impact of a bypass next to the catalysts, showing consistently higher hydrogen concentrations in the recombiner outlet. It was made sure in the final recombiner design to remove any possible bypass and maximize the number of channels available for the recombination reaction.

Finally, the experiments showed that the chimney length had to be significantly more important to have a real impact, as the medium length chimney drew performances similar to the small one's.

REFERENCES

- (s.d.). *Ansys Fluent 19.2, (2018), Theory Guide, ANSYS, Inc.*
- Meynet, N. B. (2014). Impact of oxygen starvation on operation and potential gas-phase ignition of passive auto-catalytic recombiners. *Combustion and Flame, 161 (8)*, 2192-2202.
- Reinecke, E.-A. B. (May 16–18, 2006.). First validation results of the recombiner code REKO-DIREKT. *Proc. Jahrestagung Kerntechnik, , . Aachen, Germany.*